CONF-740940--20

STUDIES OF ENERGY DEPOSITION BY NEUTRONS*

R. S. Caswell and J. J. Coyne
National Bureau of Standards
Washington, D.C. 20234

and

M. L. Randolph
Biology Division
Oak Ridge National Laboratory**
Oak Ridge, Tennessee 37830

Neutrons generate secondary particles (p, α, C, N. O, etc.) when they interact with tissue. It is through these secondary particles that nearly all of the energy deposition and biological effects occur. It is therefore of interest to determine the total energy transferred to the charged particles (kerma), the initial spectrum of the secondary particles, the slowing-down spectrum, and the details of the energy deposition by these secondary charged particles. We are continuing to study all of these quantities. Further along in the energy deposition process, one is interested in the delta-ray production cross sections and absorbed dose distributions due to the delta rays. We have not yet focused on this problem. In this report we shall discuss kerma calculations and some studies of the energy deposition in spherical volumes.

KERMA FACTORS

Kerma factors (kerma per unit fluence), sometimes called fluence-to-kerma factors, are useful in neutron dosimetry in two ways: (1) to convert kermas or absorbed doses measured in dosimeters made of approximately tissue-equivalent materials to absorbed dose in the tissue desired; and (2) to determine kerma or absorbed dose from knowledge of neutron fluence

*Supported in part by the Division of Biomedical and Environmental Research, U. S. Atomic Energy Commission.
**Operated by the Union Carbide Corporation for the U. S. Atomic Energy Commission.

and energy spectrum at the location of interest. Absorbed dose frequently can be obtained from knowledge of the kerma and the application of small corrections (see ICRU, 1969). We are carrying out kerma factor calculations for the following nuclides or elements: H, ^{6}Li, ^{7}Li, B, C, N, O, F, Na, Mg, P, S, Cl, Ar, K, Ca, Fe. The chief source of nuclear data is the Evaluated Nuclear Data File ENDF/B-4 (NNCSC, 1974) which is gradually being issued in 1974. Phosphorus is not available in this file so another file will be used. Where data is not available, reasonable assumptions from nuclear theory are made. The ENDF/B-4 data file stops at 20 MeV. In the case of hydrogen, data is available up to 30 MeV from Hopkins and Breit (1971). Between 20 and 30 MeV for other elements, some total neutron cross section data is available (Schwartz, Schrack and Heaton, 1974; Cierjacks et al, 1968), but very little else. At present it appears that the best one can do is use optical model, statistical model, and coupled-channel calculations normalized to the experimentally measured total cross section. In the higher energy region of interest to neutron therapy, 30-50 MeV, cross sections are not well enough known to make meaningful estimates of kerma factors.

In earlier work (Bach and Caswell, 1968) kerma factors were calculated for "point" energies. Where neutron cross sections are smooth, this is relatively satisfactory. However, where there are resonances and dips in cross sections, it is not completely satisfactory to tabulate kerma factors only for a specific set of point energies. Therefore, kerma factors between thermal neutron energy and 30 MeV are being calculated for 116 contiguous energy "bins", each of which is characterized by a central or average energy, E_n, and by a full bin width, ΔE_n. The cross sections used to calculate the kerma factors were averaged analytically over the energy width of the bin, using the interpolation schemes given in the

ENDF/B-4 compilation. The bin widths vary with neutron energy, and above 0.08 MeV they follow the algorithm that the bin width is 0.1 times the lower bound of each group of energies with the same bin width. Bin-averaged kerma factors were then calculated. Using these kerma factors, average kerma factors can be calculated by the user for his neutron energy spectrum.

Three computer programs are used in the calculation, with card input possible at the intermediate stages for additional data. KERMA1 reads ENDF/B-4 tapes, calculates either point or bin-averaged cross sections at the desired set of energies. KERMA2 calculates the kerma factors according to appropriate formulas, one or several elements at a time. This program is being written with provision to calculate kerma by secondary particle type, but this part is not yet complete. KERMA3 calculates kerma factors for compounds, mixtures, and tissue.

In the remainder of this section we shall compare the current results with earlier results, chiefly Bach and Caswell (1968). Other calculations have been made by Randolph (1957) at 14.1 MeV, by Auxier, Snyder, and Jones (1968), Ritts, Solomito and Stevens (1969), and Dennis (1973). We have not attempted to show comparisons to all this work as the graphs become very confusing. In Figures 1 and 2 are shown the kerma factors for hydrogen. The present calculation is based on the phase shift analysis of n-p scattering by Hopkins and Breit (1971) whereas older kerma factors were based on Gammel (1963) which did include a small anistropy in the elastic scattering. We see that the agreement is excellent. Kerma in hydrogen is probably known to 2% all the way to 30 MeV.

Kerma factors for carbon are shown in Figure 3. It is of course to be expected that the kerma factors for "point" energies will show larger excursions in value (when the energy happens to fall on a resonance or a dip

in the cross section) than the bin-averaged kerma factors. Bearing this in mind, the agreement between the older and the new cross sections is rather good, except perhaps above 15 MeV. In this particular case it is not clear that the ENDF/B-4 data is superior since all cross sections in the carbon compilation up to 20 MeV were held fixed at the values for 15 MeV. Of course the kerma increases with neutron energy under these circumstances since more energy is available to be transferred. In Figure 4 are shown kerma factors for acetylene (C_2H_2). The agreement between the old and new compilations is really excellent up to 2 MeV (better than 2 percent), and up to 15 MeV the agreement is generally good although deviations up to 6 percent sometimes appear. Above 15 MeV the agreement deteriorates to about 15% at 18 MeV, the top energy of the old compilation. Recent kerma factors reported by Dennis (1973) are in good agreement with the present calculation.

Kerma factors for nitrogen are shown in Figure 5. The overall agreement is quite good up to about 11 MeV. Above 11 MeV the new kerma factors based on ENDF/B-4 continue to rise with energy whereas the old data based chiefly on a compilation by Ray et al. (1962) go through a maximum and then decrease. The difference is primarily a real improvement in the evaluated cross sections for nitrogen by Young and Foster (1972) who realized that excited states in the residual nucleus $^{14}N^*$ from $^{14}N(n,n')^{14}N^*$ above about 9 MeV will decay primarily by proton emission which contributes very strongly to the kerma, whereas the older compilation treated the reaction as inelastic scattering which contributes relatively little to kerma. A second effect is larger estimates for the $^{14}N(n,\alpha)$ and $^{14}N(n,2\alpha)$ cross sections in the new compilation. At the higher energies most of the kerma is from (n,charged particle), (n,2α) and the (n,n'p) reactions discussed above. Interestingly the total neutron cross section and the elastic

scattering cross sections are very close in the two compilations.

Kerma factors for oxygen are shown in Figure 6. Agreement is usually within 10 percent. Again there is a slight tendency for the kerma to be higher in the new compilation due to charged-particle producing reactions.

Despite the existence of some changes in the kerma factors for the non-hydrogenous elements, if we calculate kerma factors for a four-element "wet tissue" (assumed 10% H, 12% C, 4% N, and 74% O) we find very satisfactory agreement between the new and old data even at the higher energies (see Figure 7). This is because most of the kerma is due to hydrogen for which the data is very stable.

As an example of a non-hydrogenous compound, kerma factors for CO_2 are shown in Figure 8. There are no large discrepancies between the present data and that of Bach and Caswell (1968) and Dennis (1973), although there may be a slight tendency for the new data to be higher due to better treatment of reactions leading to charged particles.

In conclusion, we believe that (1) the kerma factor data is gradually improving with time, (2) obtaining kerma factors above 20 MeV for elements other than hydrogen will be most difficult, (3) much new cross section data will be needed for reliable kerma factors above 30 MeV, and (4) for most applications the bin-averaged cross sections are most useful since the user is usually concerned with neutron spectra with significant spread in energy.

ENERGY DEPOSITION

For neutron microdosimetry, one is interested in energy deposition in certain small tissue volumes, which are usually taken as spherical. Certain averages over the energy deposition spectra are desired such as the frequency and energy averages of lineal energy ($\bar{y}_f, \bar{y}_D$) or their equivalent specific energy parameters (z_1, ζ). Calculations of these parameters have been made as a function of neutron energy.

The energy and angular dependence of the required neutron cross sections are taken from the ENDF/B data file or from other sources. These cross sections are used to calculate the initial spectra of charged particles produced by a given energy neutron (Caswell and Coyne, 1972). Experimental stopping powers are then folded into these "initial spectra" to give the "slowing-down" spectra of the charged particles. These two spectra are then combined with chord length distributions for the cavity and the integrations over the possible chord lengths are done numerically on the computer.

In order to check this computer code and also to help illuminate the influence of the various factors entering the calculations, a simple model has been developed. First it is assumed that at a given energy only one reaction is important for a given charged particle and the angular dependence of this reaction is isotropic. Then we assume that the stopping power in the medium has one of the following three simple energy variations:

$$\text{I} \quad \text{S.P.} = A \qquad \text{II} \quad \text{S.P.} = a\sqrt{E} \qquad \text{III} \quad \text{S.P.} = B/E \,.$$

Using these simplifying assumptions all of the required integrals can be performed analytically. In order to compare with the actual calculations three constants must be determined. These constants are picked using information from the initial and slowing-down spectra, so that none of the cavity integrations are involved.

The constant value of the assumed initial spectrum, η_p and the maximum energy of the charged particle, $\mathcal{E}_M$, are chosen so that

$$\int_0^{E_M} N_p(E)dE(\text{Actual}) = \int_0^{E_M} \eta_p dE = \eta_p \mathcal{E}_M$$

and

$$\int_0^{E_M} E \cdot N_p(E)dE(\text{Actual}) = \int_0^{E_M} \eta_p E dE = \frac{\eta_p \mathcal{E}_M^2}{2} \,.$$

The third constant is the one used in the stopping power. It is chosen so that

$$\int_0^{E_M} N_R(E)dE(\text{Actual}) = \int_0^{\mathcal{E}_M} \frac{1}{S.P.} \int_E^{\mathcal{E}_M} \eta_p dE' \, dE = \eta_p \int_0^{\mathcal{E}_M} \frac{\mathcal{E}_M - E}{S.P.} dE \ .$$

When the constants are fixed in this way, the value for $\bar{E}_f$ or $\bar{y}_f$ will be the same for the three models and for the actual calculations. In order to compare results we must compare the values of $\bar{E}_D$ or $\bar{y}_D$ or the equivalent ζ. Figure 9 gives the comparison for protons and Figure 10 gives a similar comparison for oxygen ions. It must be remembered that the evaluation of $\bar{E}_D$ for the actual calculations involves a long computer calculation at each energy. For the three models, $\bar{E}_D$ is simple to calculate once the initial and slowing-down spectra are known.

Figures 11 and 12 are based on the results of the actual calculations. Figure 11 shows that the $\bar{E}_f$ (total), when all charged particles are included, differs only slightly from $\bar{E}_f$ for protons alone. Note that $\bar{E}_f$ (total) equals $\bar{E}_f$ (protons) times the percentage of the total events due to protons plus the $\bar{E}_f$ for the n^{th} charged particle times the percentage due to this charged particle, etc. Figure 12 is a similar plot for $\bar{E}_D$ but now the values for the various charged particles are weighted by the percentage of the kerma. This figure can be compared with Fig. 12 of Kellerer and Rossi (1972), where they point out that the effective value of $\bar{y}_D$ will be modified by saturation.

REFERENCES

1. Auxier, J. A., W. S. Snyder, and T. D. Jones (1968). Neutron interactions and penetration in tissue. In Attix, Roesch, and Tochilin, Radiation Dosimetry, Vol. I, Academic Press, New York and London, 275.

2. Bach, R. L. and R.S. Caswell (1968). Radiation Research 35, 1.

3. Caswell, R. S. and J. J. Coyne (1972). Radiation Research 52, 448.

4. Cierjacks, S., P. Forti, D. Kopsch, L. Kropp, J. Nebe and H. Unseld (1968). High resolution total neutron cross sections between 0.5 - 30 MeV. Kernforschungszentrum Karlsruhe Report KFK 1000.

5. Dennis, J. A. (1973). Phys. Med. Biol. 18, 379

6. Hopkins, J. C. and G. Breit (1971). Nuclear Data Tables A9, 137.

7. International Commission on Radiation Units and Measurements, ICRU (1969). Neutron fluence, neutron spectra, and kerma. Report No. 13.

8. Kellerer, A. M. and H. H. Rossi (1972). Current topics in Radiation Research Quarterly 8, 85.

9. NNCSC (1974). Evaluated Nuclear Data File ENDF/B, Version IV. Prepared by the National Neutron Cross Section Center, Brookhaven National Laboratory, Upton, New York.

10. Randolph, M. L. (1957). Radiation Research 7, 47.

11. Ray, J. H., E. S. Troubetzkoy, M. H. Kalos, N. Tralli, A. J. Longano, R. P. Sullivan and B. H. Trupin (1962). Fast neutron cross sections for titanium, potassium, magnesium, nitrogen, aluminum, silicon, sodium, oxygen, and manganese. NDL-TR-30 (UND-5002), U. S. Army Chemical Corps, Nuclear Defense Laboratory, Army Chemical Center, Edgewood, Maryland.

12. Ritts, J. J., M. Solomito and P. N. Stevens (1969). Nuclear Applications and Technology 7, 89.

13. Schwartz, R. B., R. A. Schrack, and H. T. Heaton, II (1974). MeV Total Neutron Cross Sections. National Bureau of Standards (U.S.) Monograph 138.

14. Young, P. G. and D. G. Foster (1972). An evaluation of the neutron and gamma-ray production cross sections for nitrogen. U. S. Atomic Energy Commission Report LA-4725.

FIGURE CAPTIONS

1. Kerma factors for hydrogen from 0.1 to 1 MeV. Present bin-averaged kerma factors are from the ENDF/B-4 compilation and are based on Hopkins and Breit (1971). The "point" energy kerma factors are from the older compilation, Bach and Caswell (1968).

2. Kerma factors for hydrogen from 1 to 30 MeV. Present kerma factors based on Hopkins and Breit (1971) are compared to Bach and Caswell (1968).

3. Kerma factors for carbon, 0.1 to 20 MeV. Present kerma factors based on ENDF/B-4 are compared to Bach and Caswell (1968).

4. Kerma factors for acetylene, 0.1 to 20 MeV. Present kerma factors based on ENDF/B-4 are compared to Bach and Caswell (1968) using proper composition by weight. Above 2 MeV a comparison is made to kerma factors of Dennis (1973) (See insert).

5. Kerma factors for nitrogen. Present kerma factors based on ENDF/B-4 are compared to Bach and Caswell (1968).

6. Kerma factors for oxygen. Present kerma factors based on ENDF/B-4 are compared to Bach and Caswell (1968).

7. Kerma factors for "wet tissue", chosen to make an identical comparison between the present kerma factors based on ENDF/B-4 and the data of Bach and Caswell (1968). The assumed composition is 10% H, 12% C, 4% N, and 74% O by weight.

8. Kerma factors for CO_2. Present calculation is compared to the data of Bach and Caswell (1968) and Dennis (1973).

9. Dose-mean energy deposition $\bar{E}_D$ for protons in ICRU muscle tissue as a function of neutron energy from detailed calculations and three models.

10. Dose-mean energy deposition $\bar{E}_D$ for oxygen ions in tissue as a function of neutron energy.

11. Frequency-mean energy deposition $\bar{E}_f$ for protons and all particles in tissue as a function of neutron energy. Scale on right refers to the percentage of total events.

12. Dose-mean energy deposition $\bar{E}_D$ for protons and all particles in tissue as a function of neutron energy. Scale on right refers to percentage of kerma.

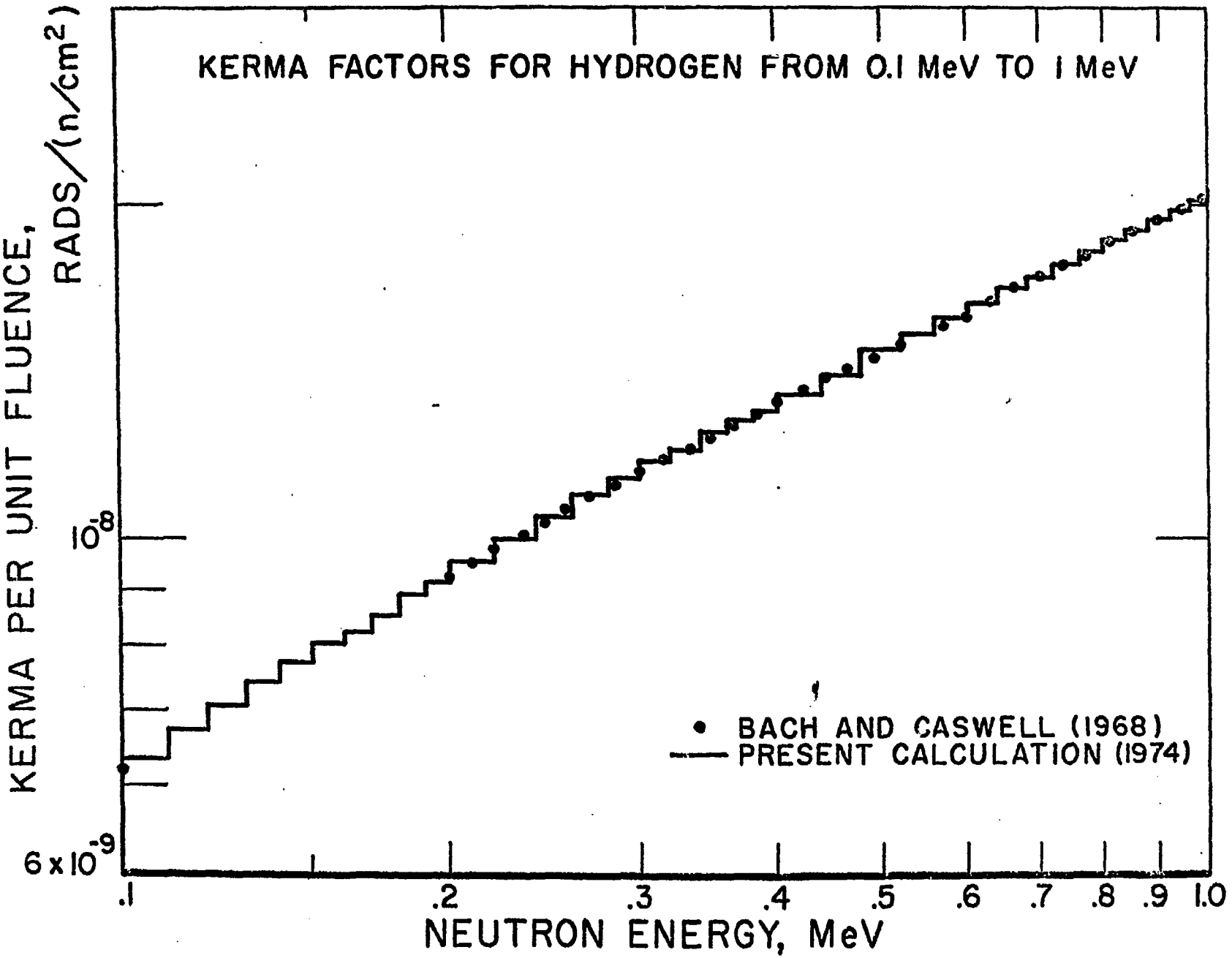
KERMA FACTORS FOR HYDROGEN FROM 0.1 MeV TO 1 MeV
KERMA PER UNIT FLUENCE, RADS/(n/cm²)
10⁻⁸
6 x 10⁻⁹
.1
.2
.3
.4
.5
.6
.7
.8
.9
1.0
NEUTRON ENERGY, MeV
BACH AND CASWELL (1968)
PRESENT CALCULATION (1974)

FIGURE 1

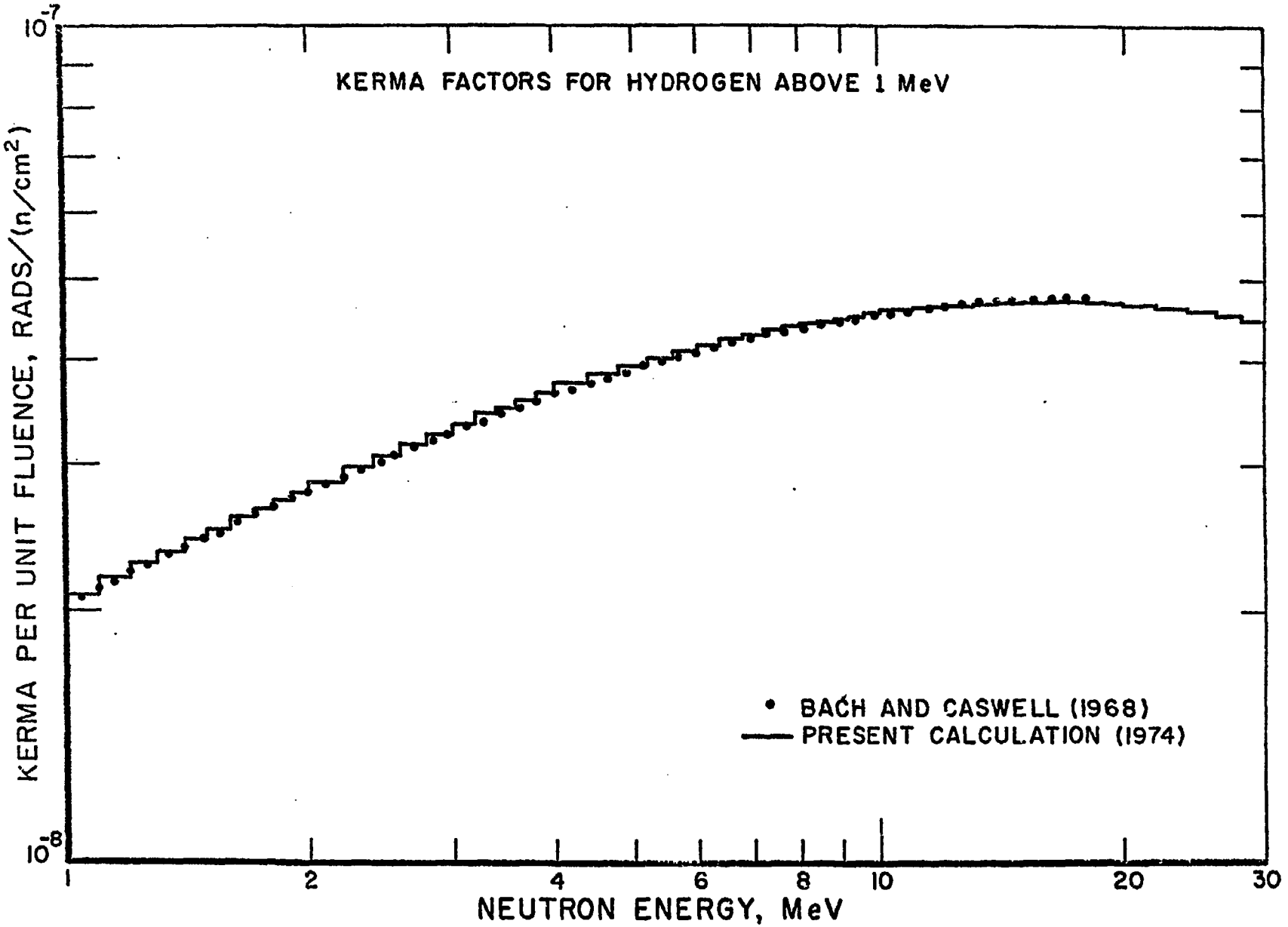
KERMA FACTORS FOR HYDROGEN ABOVE 1 MeV
KERMA PER UNIT FLUENCE, RADS/(n/cm²)
10⁻⁷
10⁻⁸
1
2
4
6
8
10
20
30
NEUTRON ENERGY, MeV
• BACH AND CASWELL (1968)
— PRESENT CALCULATION (1974)

FIGURE 2

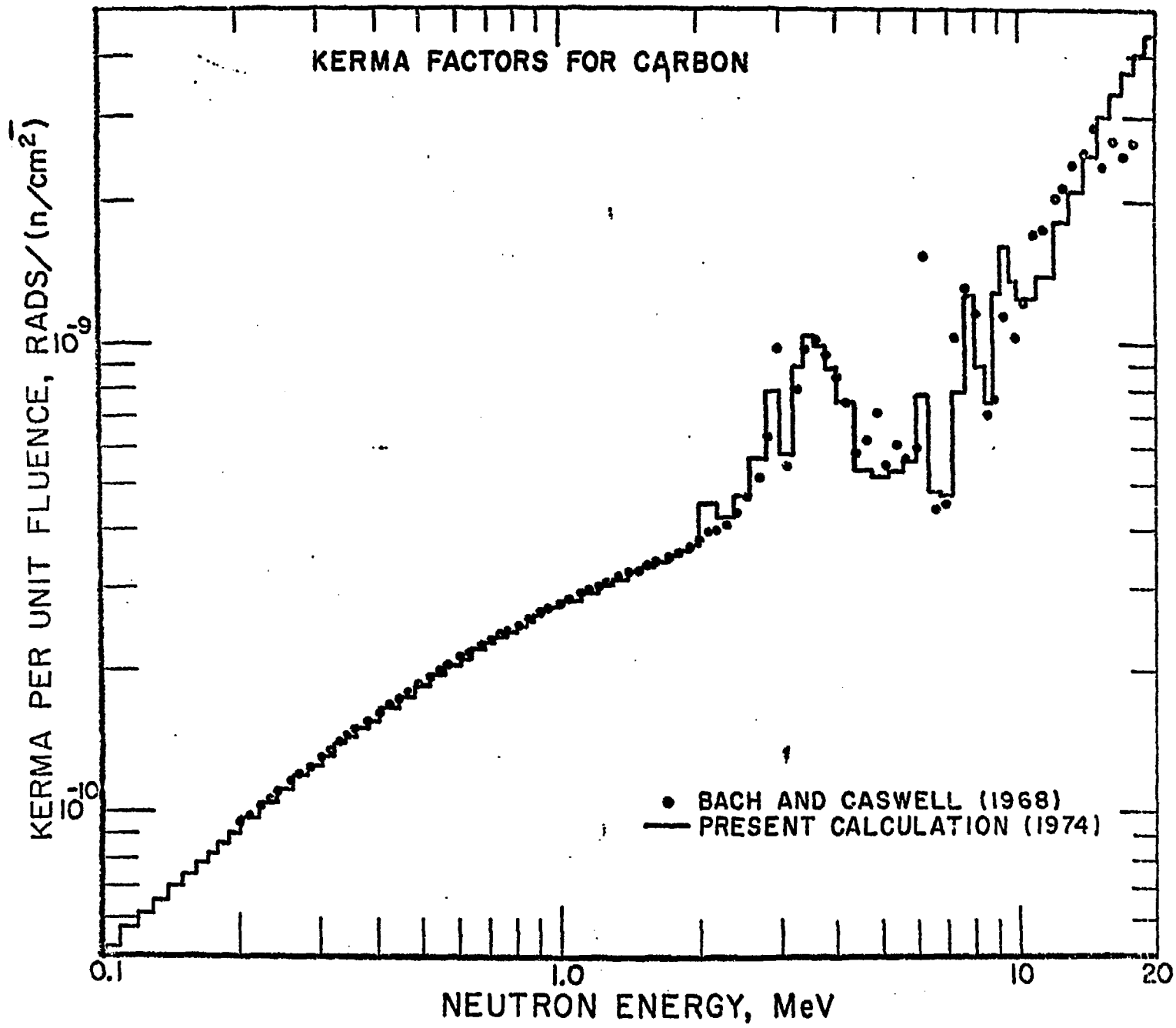
KERMA FACTORS FOR CARBON
KERMA PER UNIT FLUENCE, RADS/(n/cm²)
10⁻⁹
10⁻¹⁰
0.1
1.0
10
20
NEUTRON ENERGY, MeV
BACH AND CASWELL (1968)
PRESENT CALCULATION (1974)

FIGURE 3

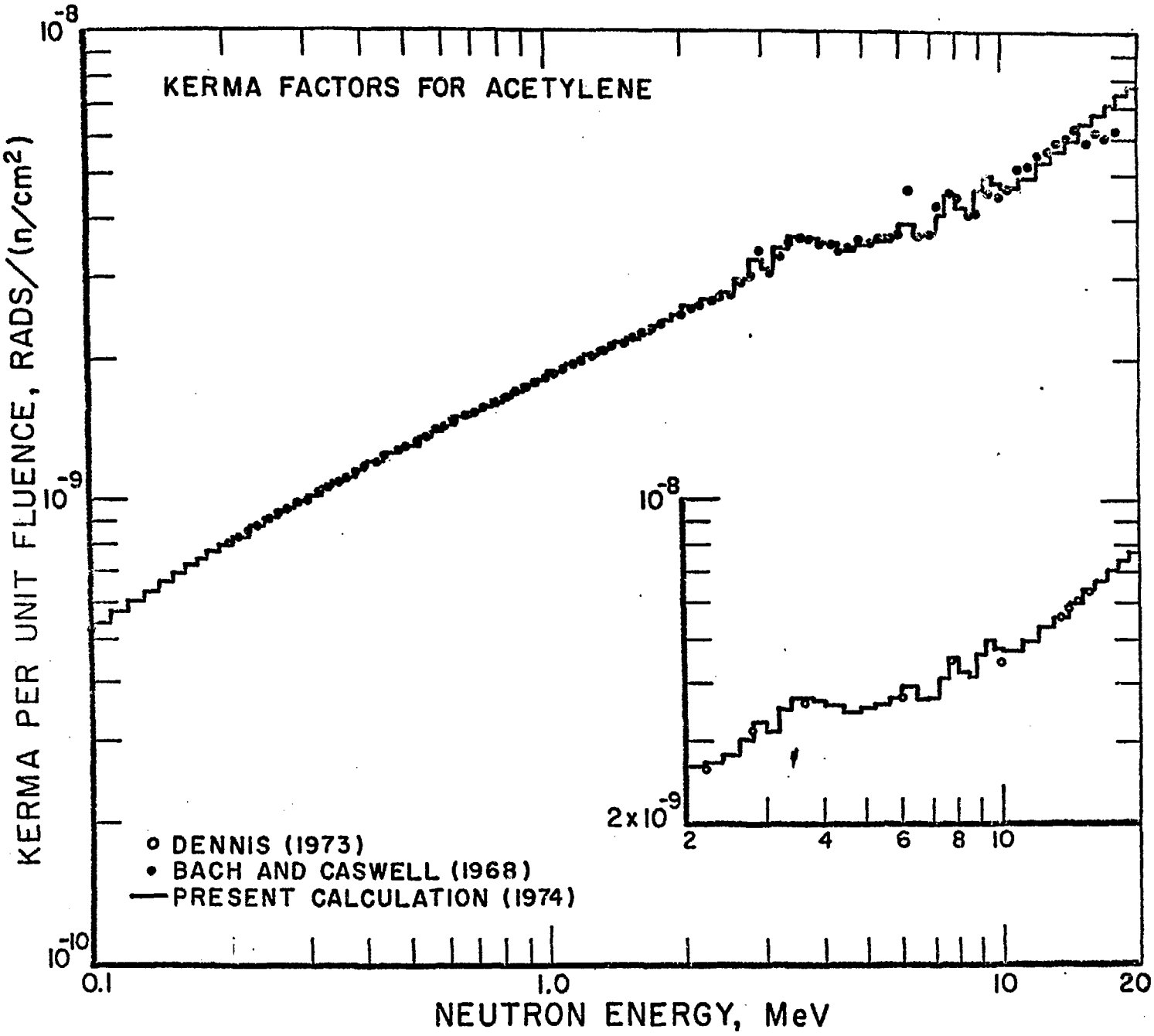
KERMA FACTORS FOR ACETYLENE
KERMA PER UNIT FLUENCE, RADS/(n/cm²)
NEUTRON ENERGY, MeV
10⁻⁸
10⁻⁹
10⁻¹⁰
0.1
1.0
10
20
2x10⁻⁹
2
4
6
8
10
o DENNIS (1973)
• BACH AND CASWELL (1968)
—PRESENT CALCULATION (1974)

FIGURE 4

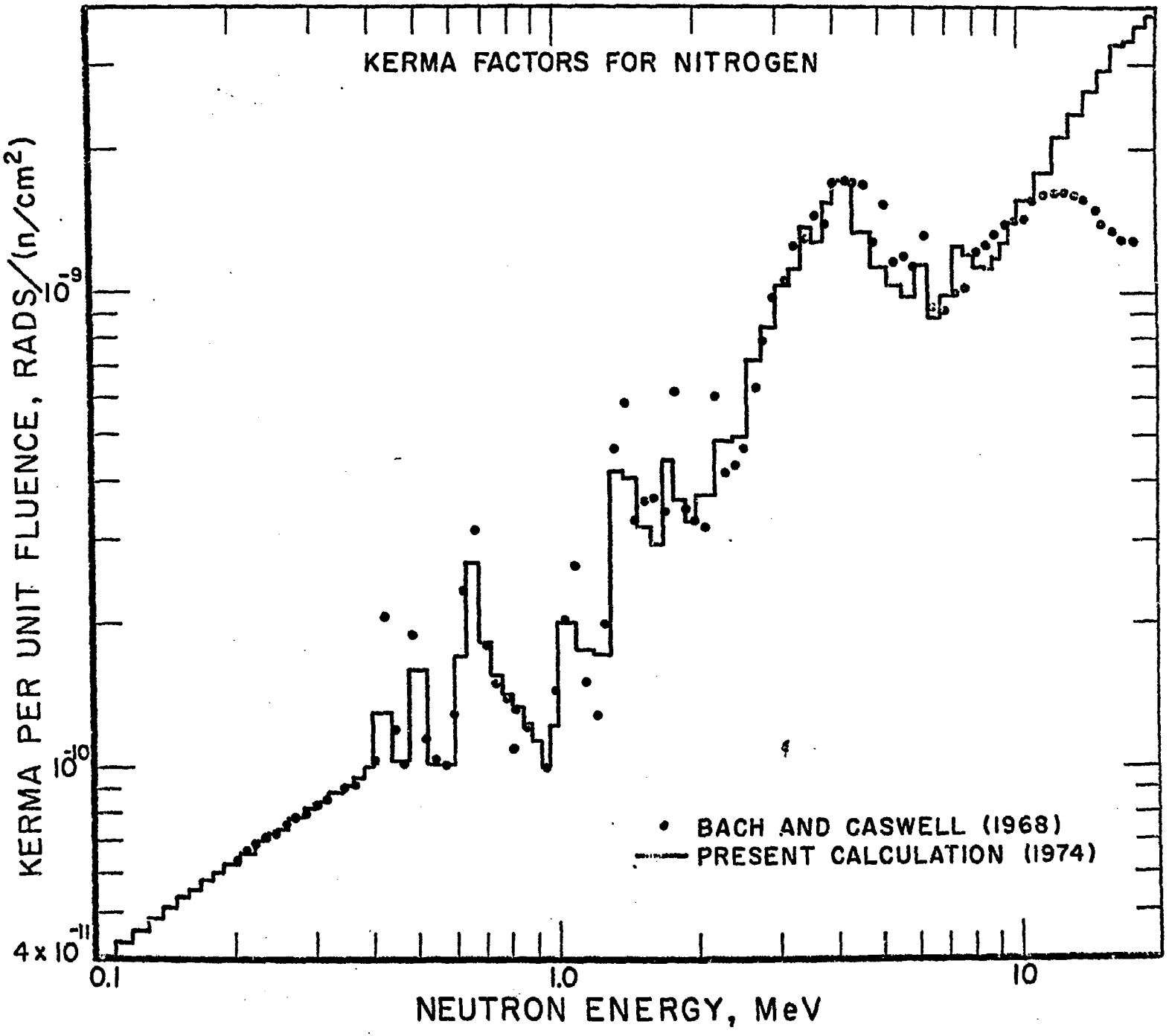
KERMA FACTORS FOR NITROGEN
KERMA PER UNIT FLUENCE, RADS/(n/cm²)
10⁻⁹
10⁻¹⁰
4 x 10⁻¹¹
0.1
1.0
10
NEUTRON ENERGY, MeV
BACH AND CASWELL (1968)
PRESENT CALCULATION (1974)

FIGURE 5

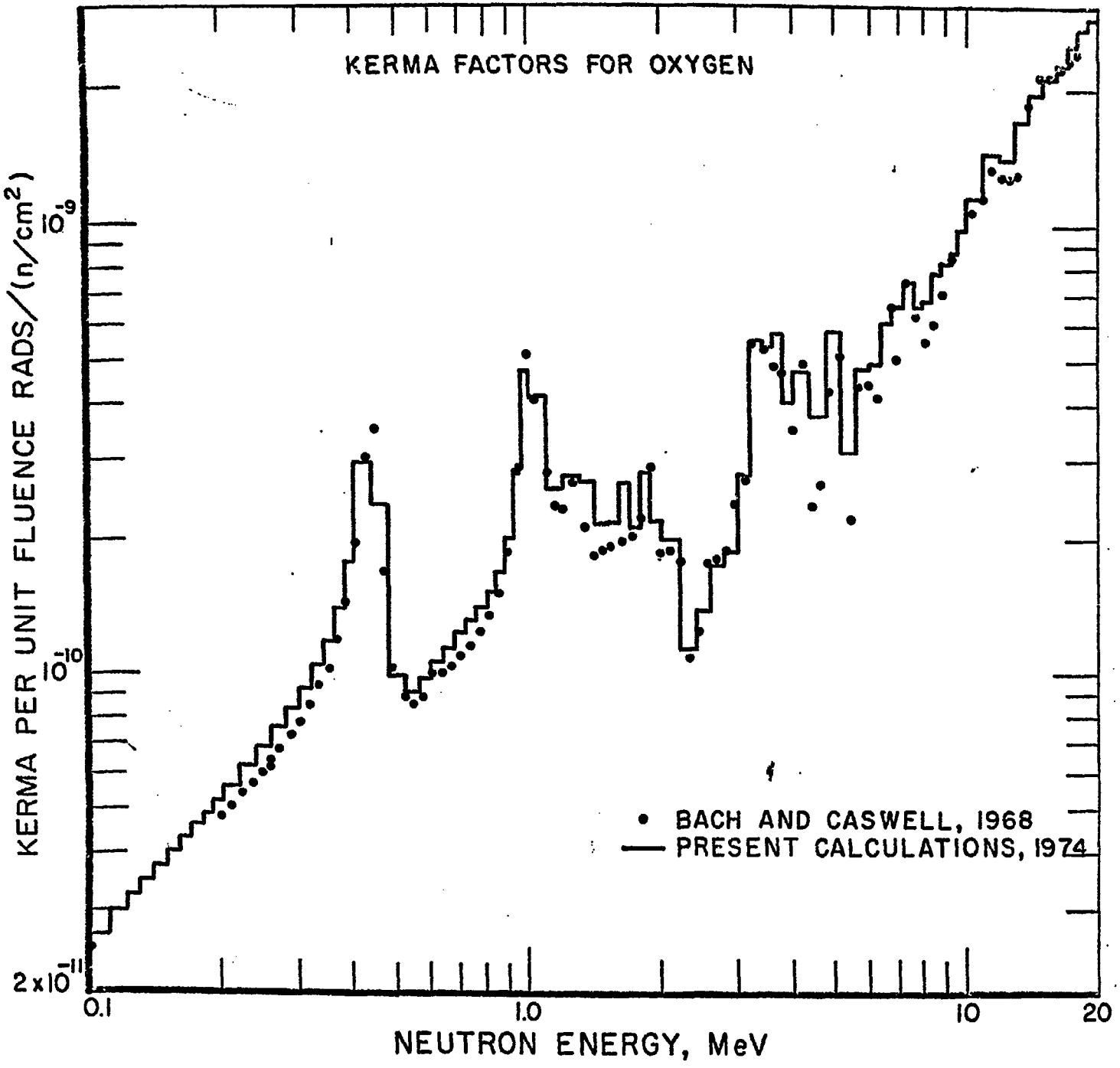
KERMA FACTORS FOR OXYGEN
KERMA PER UNIT FLUENCE RADS/(n/cm²)
10⁻⁹
10⁻¹⁰
2x10⁻¹¹
0.1
1.0
10
20
NEUTRON ENERGY, MeV
BACH AND CASWELL, 1968
PRESENT CALCULATIONS, 1974

FIGURE 6

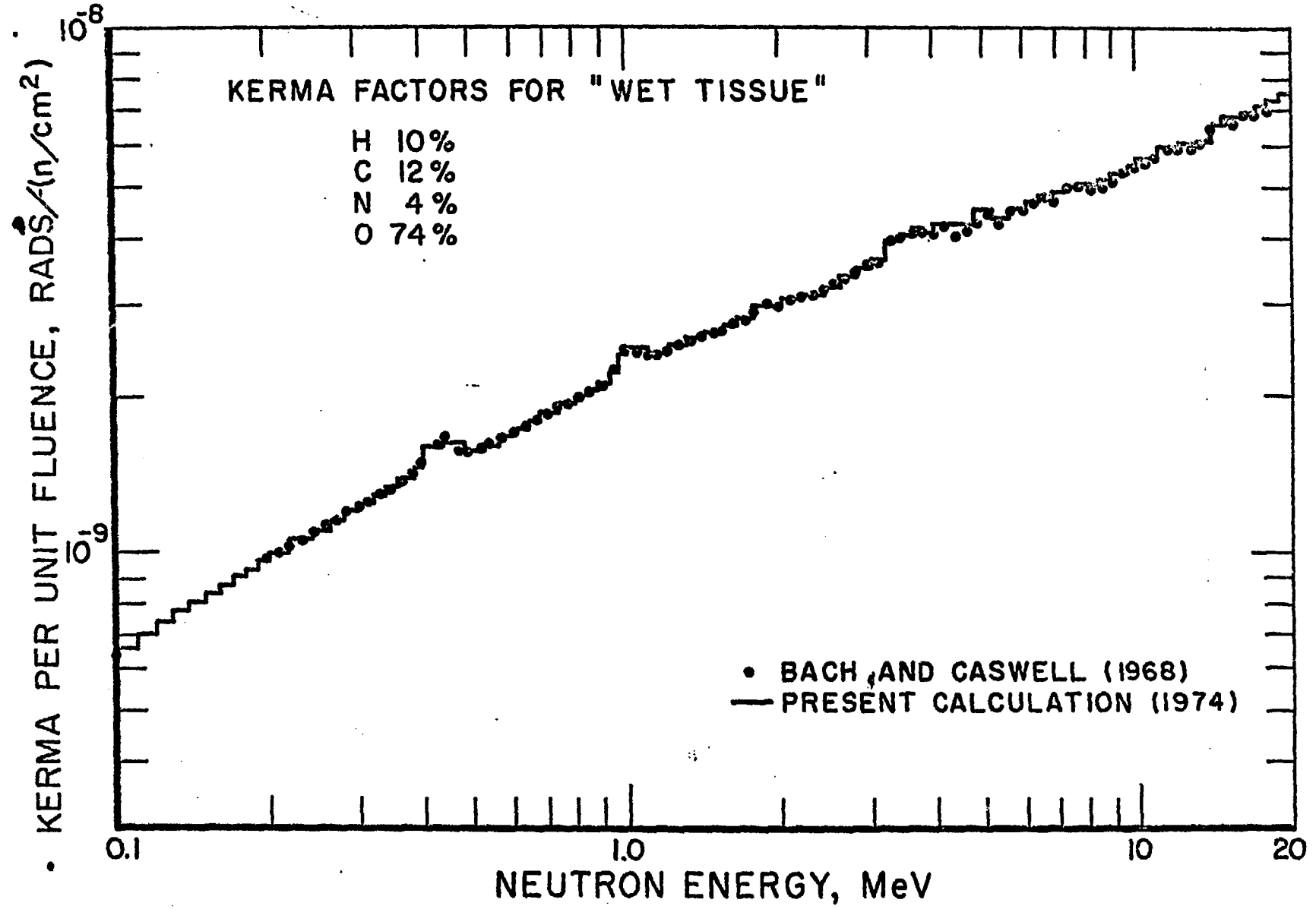
KERMA FACTORS FOR "WET TISSUE"
H 10%
C 12%
N 4%
O 74%
• BACH AND CASWELL (1968)
— PRESENT CALCULATION (1974)
• KERMA PER UNIT FLUENCE, RADS/(n/cm²)
10⁻⁸
10⁻⁹
0.1
1.0
10
20
NEUTRON ENERGY, MeV

FIGURE 7

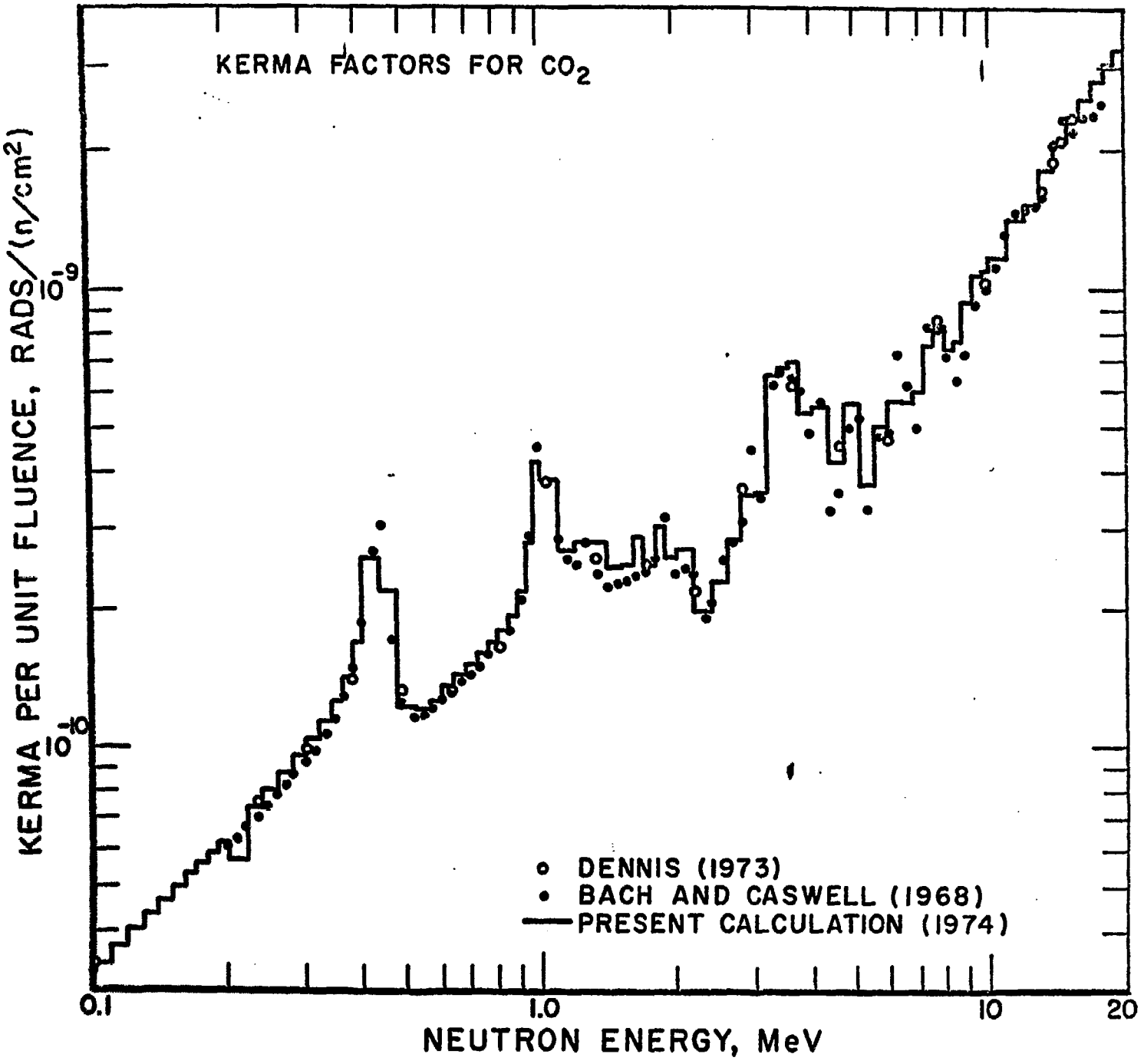
KERMA FACTORS FOR CO_2
KERMA PER UNIT FLUENCE, RADS/(n/cm²)
0.1
1.0
10
20
NEUTRON ENERGY, MeV
DENNIS (1973)
BACH AND CASWELL (1968)
PRESENT CALCULATION (1974)

FIGURE 8

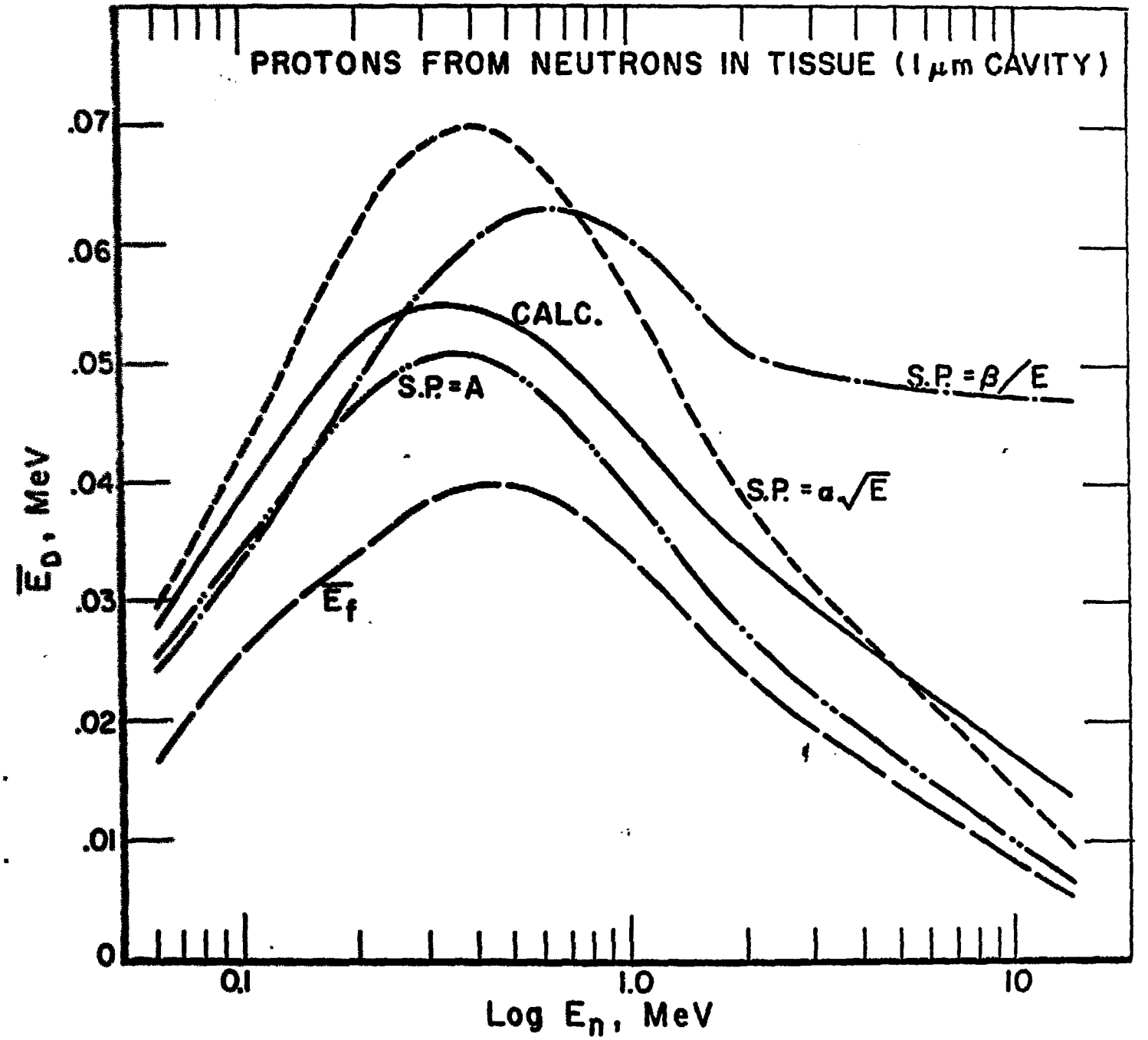
PROTONS FROM NEUTRONS IN TISSUE (1 μm CAVITY)
.07
.06
.05
.04
.03
.02
.01
0
$\bar{E}_D$, MeV
CALC.
S.P. = A
S.P. = β/E
S.P. = α√E
$\bar{E}_f$
0.1
1.0
10
Log E_n, MeV

FIGURE 9

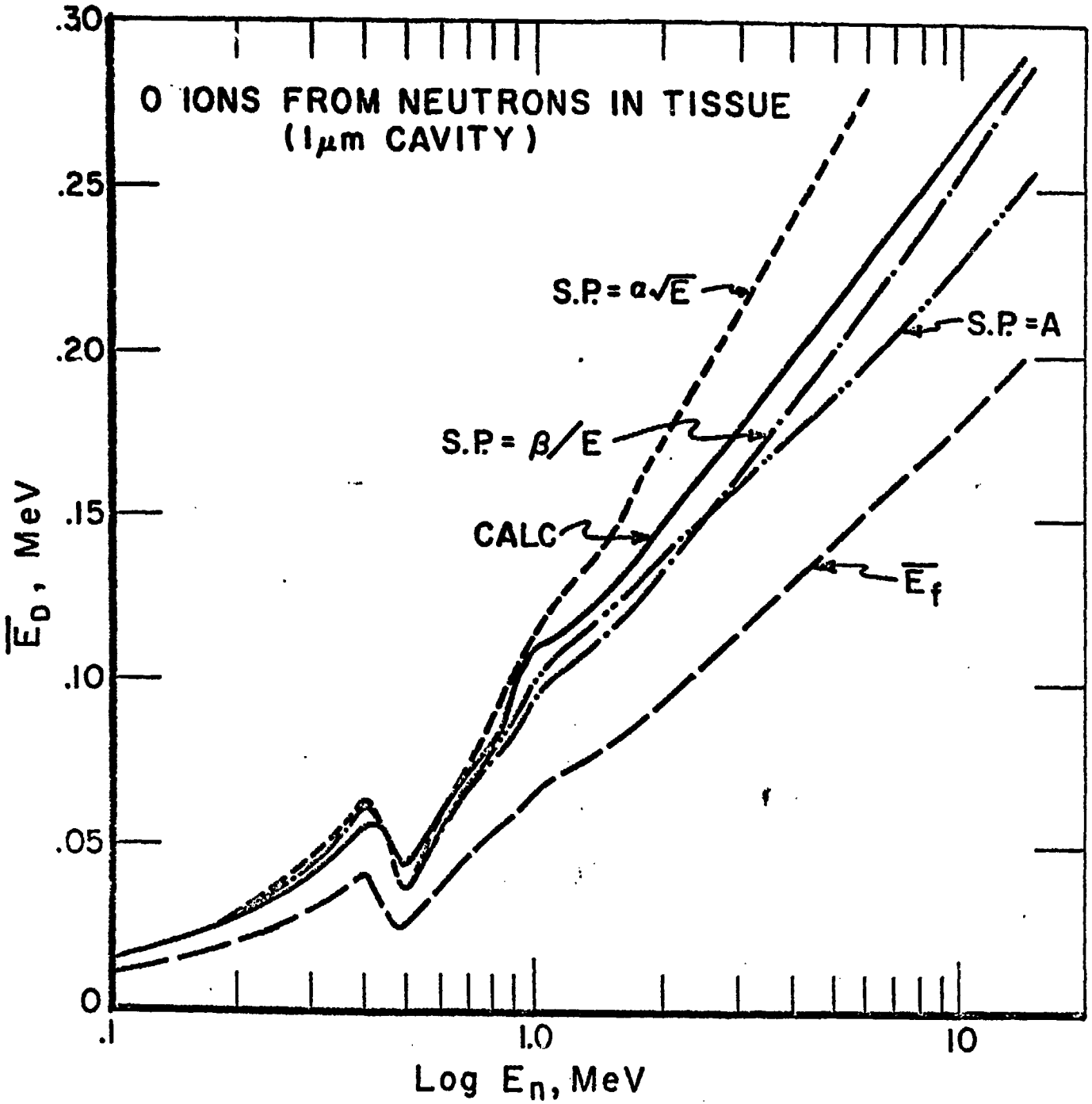
O IONS FROM NEUTRONS IN TISSUE
(1μm CAVITY)
S.P. = a√E
S.P. = β/E
CALC
S.P. = A
$\overline{E}_f$
$\overline{E}_D$, MeV
Log E_n, MeV
.30
.25
.20
.15
.10
.05
0
.1
1.0
10

FIGURE 10

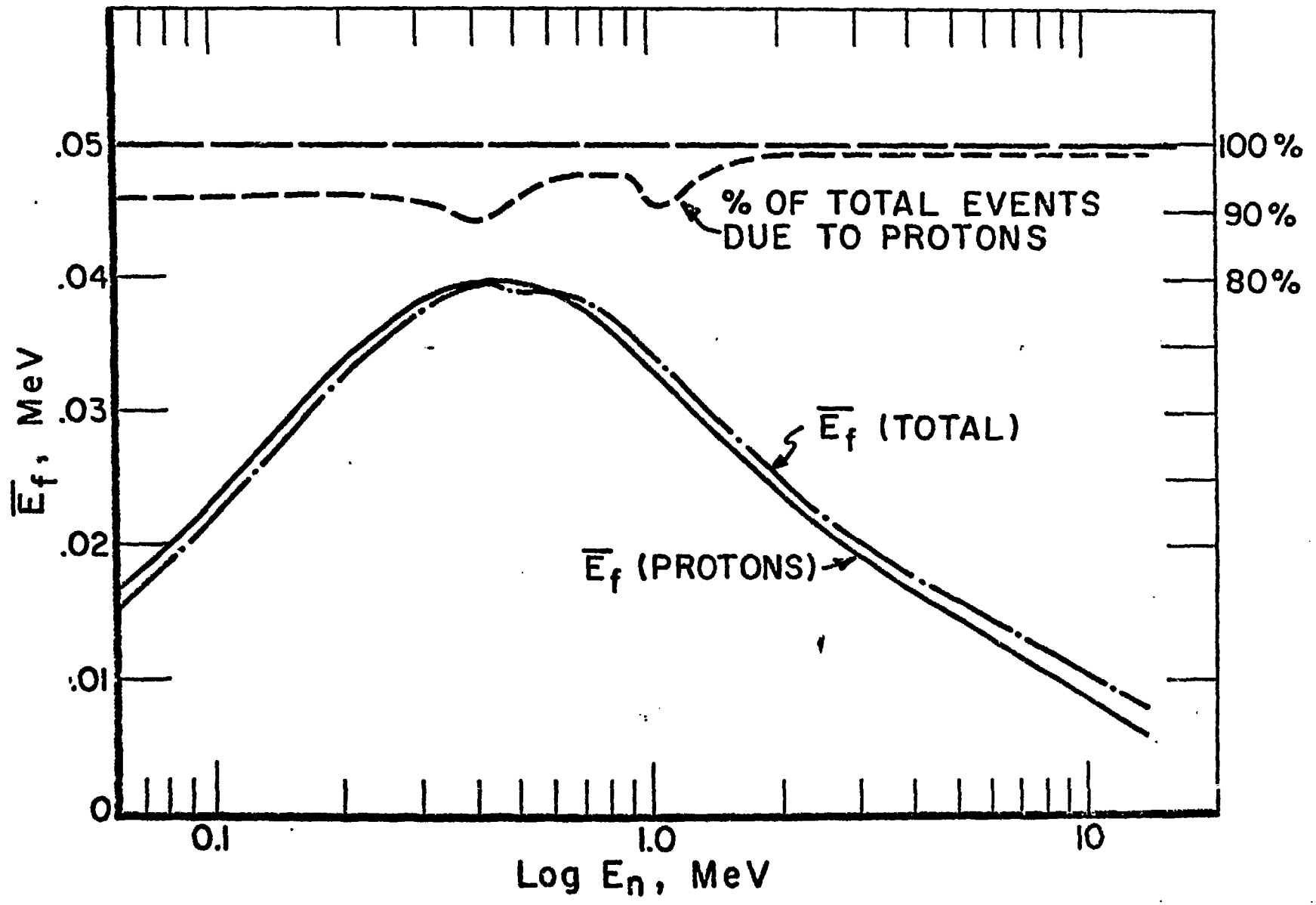
.05
.04
.03
.02
.01
0
$\overline{E_f}$, MeV
100%
90%
80%
% OF TOTAL EVENTS
DUE TO PROTONS
$\overline{E_f}$ (TOTAL)
$\overline{E_f}$ (PROTONS)
0.1
1.0
10
Log E_n, MeV

FIGURE 11

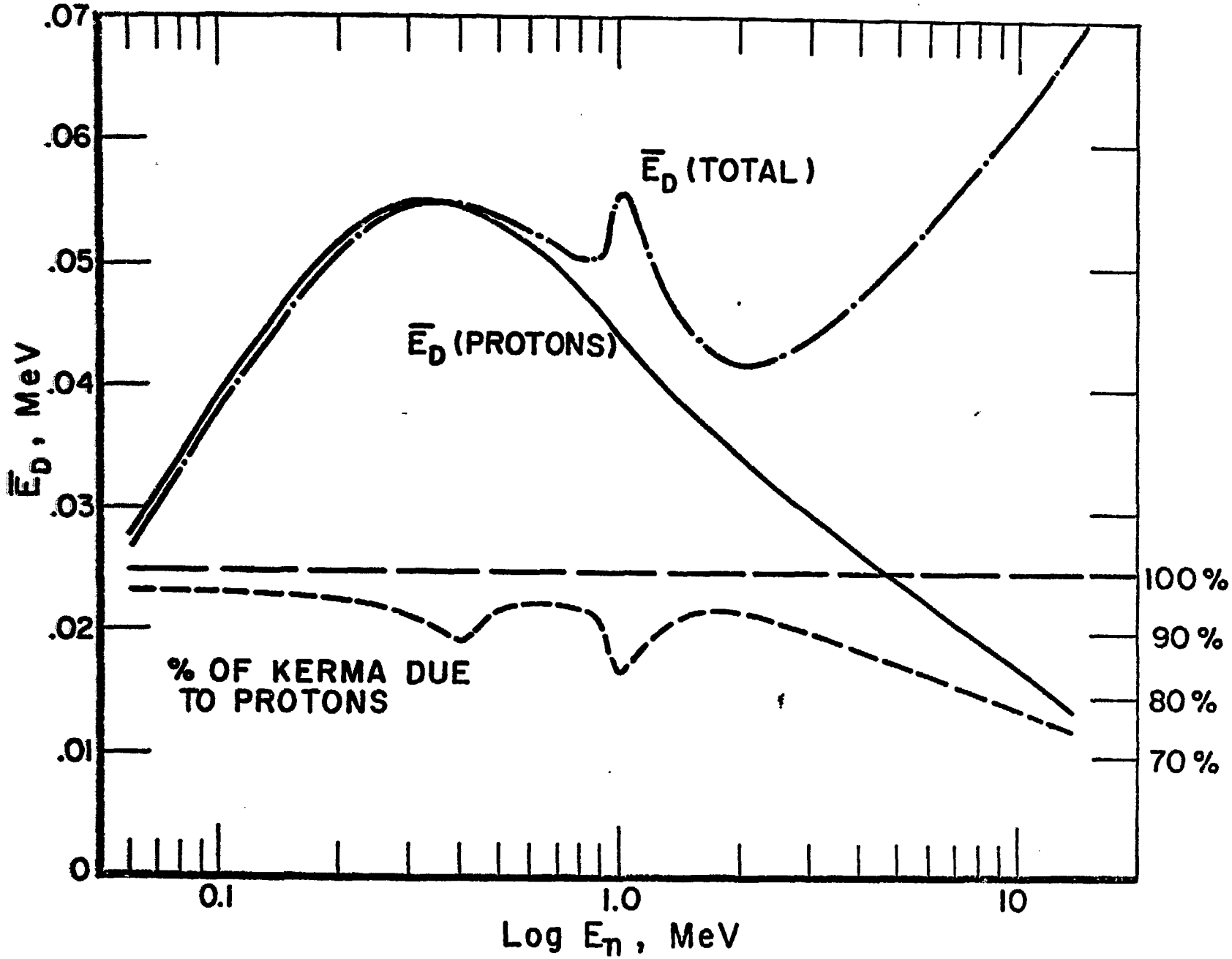
.07
.06
.05
.04
.03
.02
.01
0
$\bar{E}_D$, MeV
$\bar{E}_D$ (TOTAL)
$\bar{E}_D$ (PROTONS)
% OF KERMA DUE TO PROTONS
100 %
90 %
80 %
70 %
0.1
1.0
10
Log E_n, MeV

FIGURE 12